Supplemental Data for "Ion Competition in Condensed DNA Arrays in the Attractive Regime"

Xiangyun Qiu[1,*], John Giannini[2], Steven C Howell[1], Qi, Xia[1], Fuyou Ke[1], and Kurt Andresen[2,*]

[1]*Department of Physics, George Washington University, Washington, DC, 20052*

[2]*Department of Physics, Gettysburg College, Gettysburg PA, 17325*

**To whom correspondence should be addressed:*

Tel: 1.202.994.6537; Email: xqiu@gwu.edu or kandrese@gettysburg.edu

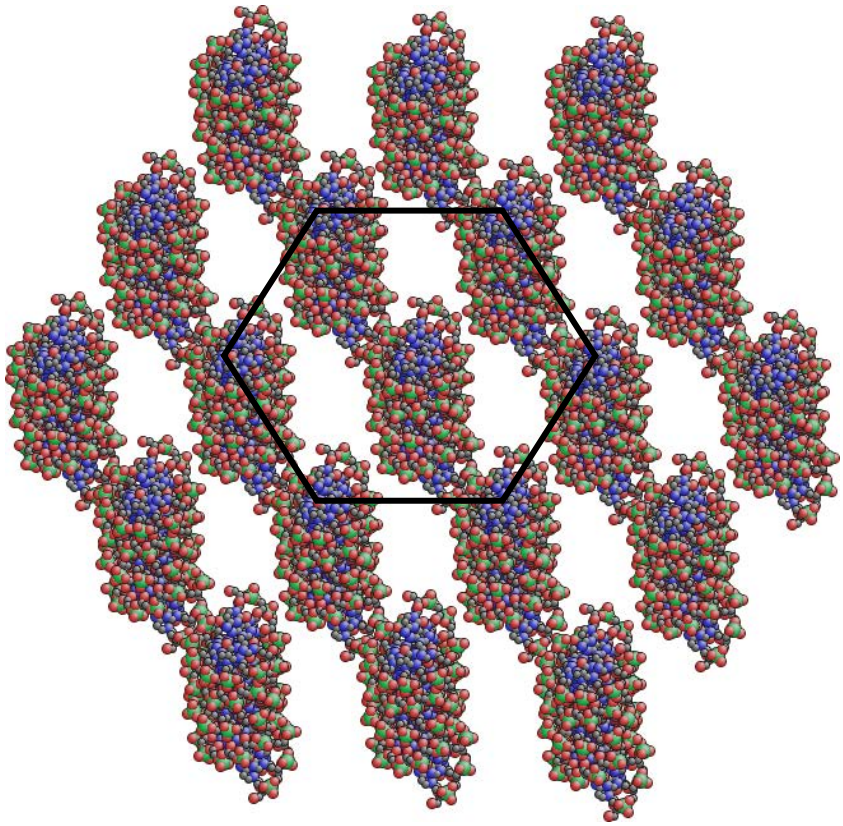

Figure S1. Another view of the DNA array used in the Adaptive Poisson-Boltzmann Solver (APBS) calculation. The DNA array is made up of nineteen 24-base-pair DNA duplexes.

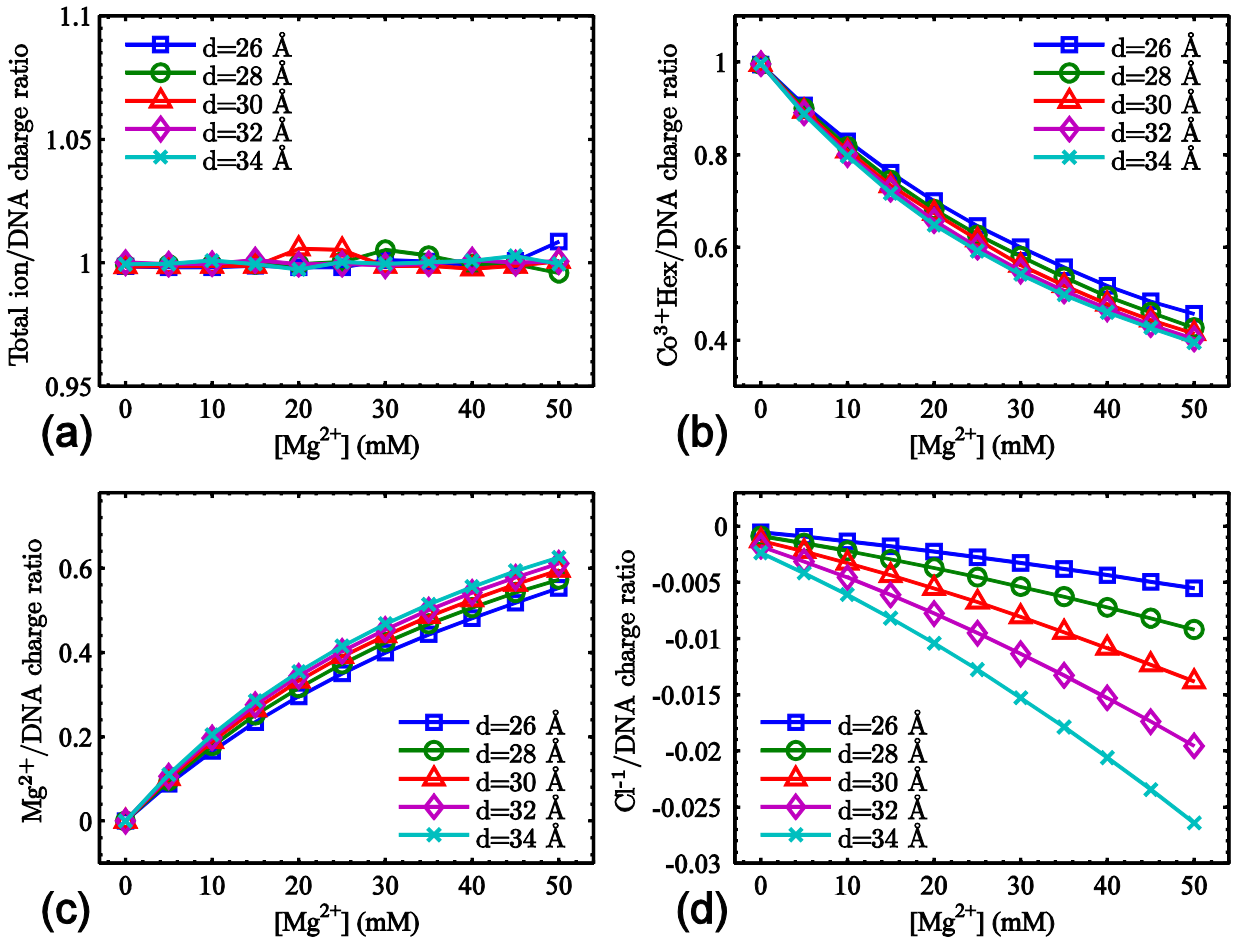

Figure S2. The effects of the cell radius on the results of the cylindrical cell model (CCM). DNA is treated as a 10-Å-radius cylinder with a linear charge density of -2/3.4 e/Å. The salt conditions are the fixed [Co^{3+}Hex] of 5 mM and varied [Mg^{2+}]s from 0 to 50 mM. Each curve represents one series of calculations under a constant cell radius (i.e., the DNA-DNA spacing d) indicated by the legend. (a) The total ion/DNA charge ratio ($3n_{Co}+2n_{Mg}-n_{Cl}$). The expected charge neutrality is observed. (b) The Co^{3+}Hex/DNA charge ratios ($3n_{Co}$). (c) The Mg^{2+}/DNA charge ratio ($2n_{Mg}$). (d) The Cl^{-1}/DNA charge ratio ($-1n_{Cl}$), noting the negative sign. The general trend indicates the decrease of $3n_{Co}$ and the increases of $2n_{Mg}$ and n_{Cl} upon increasing the DNA-DNA spacing. This can be attributed to the weakening of the electrostatic field in the interstitial space which weakens the electrostatic coupling with cations of higher valences to a larger extent. Nonetheless, a 2-Å change of the DNA-DNA spacing (~15% volume change) leads to rather small differences that are insignificant compared with the differences discussed in the main text.

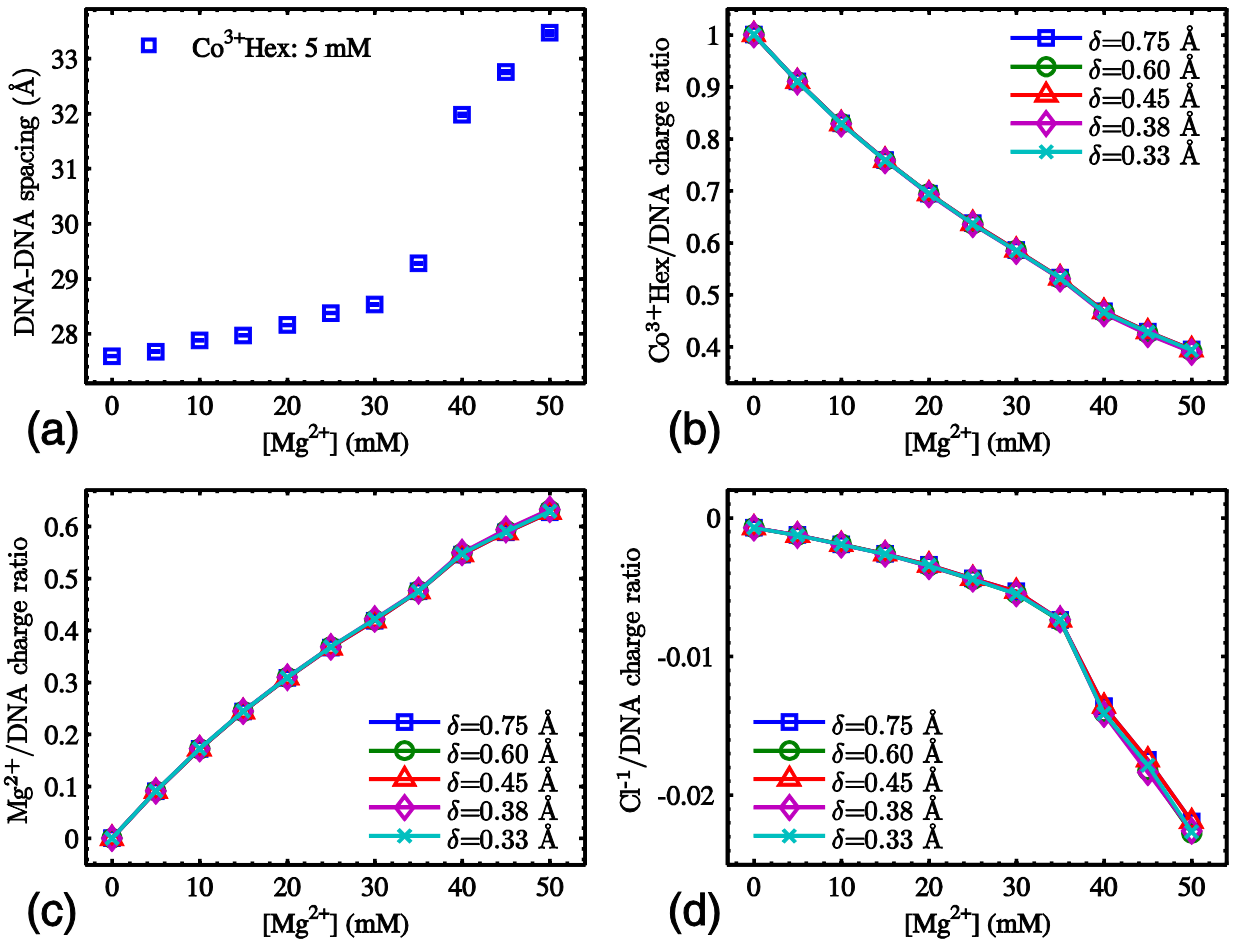

Figure S3. Validity of the grid size of 0.45 Å for the APBS calculation. As described in the main text, the APBS box has a dimension of 225×225×150 Å with a DNA array in the center as shown in Suppl. Fig. S1. The salt conditions are the fixed [Co^{3+}Hex] of 5 mM and varied [Mg^{2+}]s from 0 to 50 mM, and all ionic radii are 2 Å. (a) The measured DNA-DNA spacing of the DNA array used for the APBS calculations. (b) The Co^{3+}Hex/DNA charge ratio ($3n_{Co}$) as a function of [Mg^{2+}] for different grid sizes indicated by the legends. (c) The Mg^{2+}/DNA charge ratio ($2n_{Mg}$). (d) The Cl^{-1}/DNA charge ratio ($-1n_{Cl}$). Note that it carries a negative sign and the decrease indicates an increase in its absolute value. Adding the three curves together gives exact unity (not shown), as expected from overall charge neutrality $3n_{Co}+2n_{Mg}-n_{cl}=1$. Above all, the curves shown in (b)-(d) are virtually identical at all grid sizes, except that the $-n_{Cl}$ (d) shows small variations at highest Mg^{2+} concentrations. The choice of the grid size of 0.45 Å is thus validated.

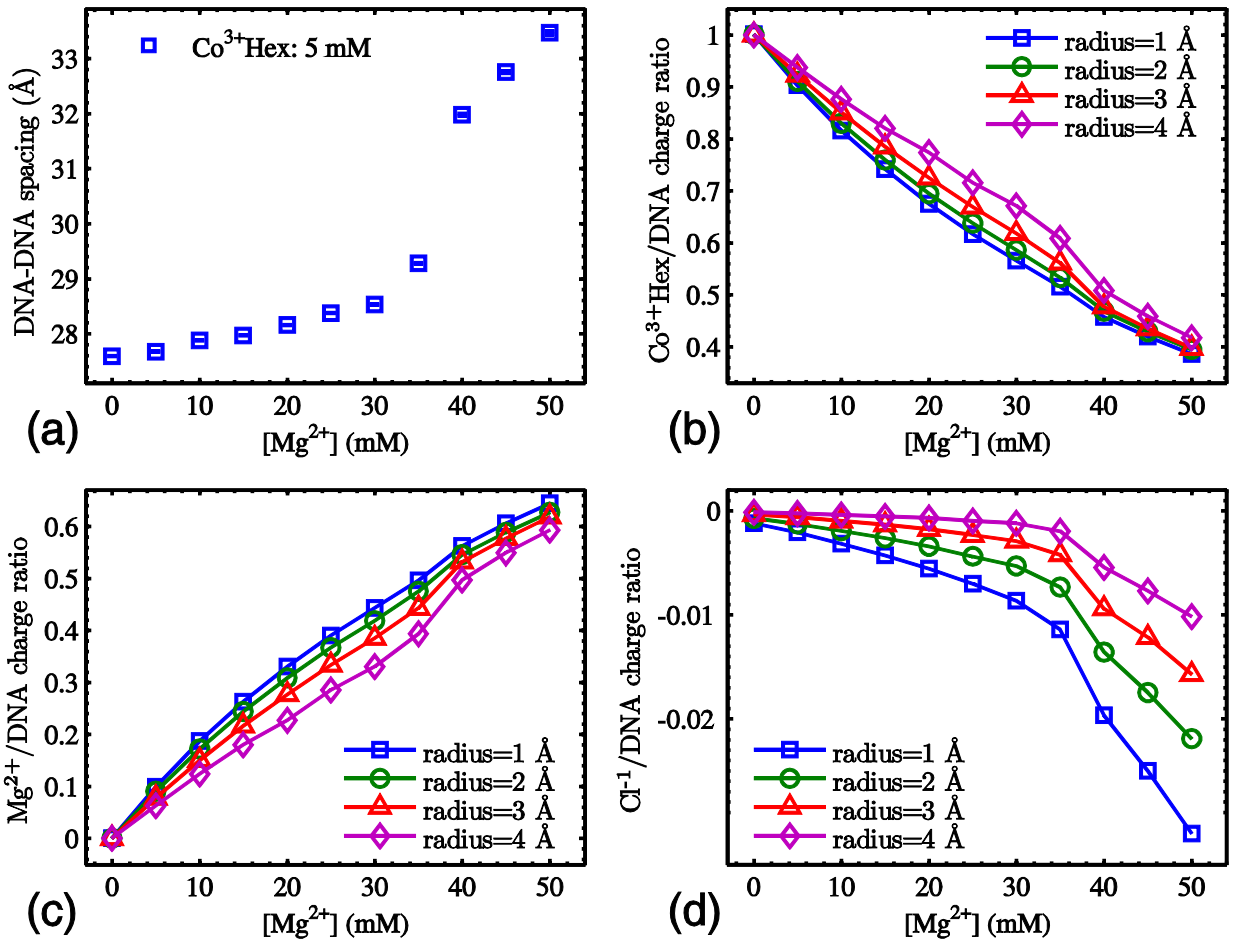

Figure S4. The effects of the ionic radius on the APBS calculation. The parameters are identical to Suppl. Fig. S3 except that all calculations are with the same grid size (0.45 Å) but varied ionic radii from 1 to 4 Å. For brevity, (a)-(d) show the same calculated results as in Suppl. Fig. S3a-d, but for different ion radii indicated by the legends. As the primary effect of the ionic radius is to define the ion accessible volume in APBS calculations, increasing the ionic radii effectively compresses the interstitial ions into smaller spaces. This increases the electrostatic fields in the ion-occupied spaces and thus favors the ions of higher valences. In accord, the results shown in (b)-(d) indicate noticeable increases of Co^{3+}Hex and decreases of Mg^{2+} and Cl^{-} as the ion radii are increased. Given the dependences on the ionic radius, it is important to choose proper values but this is non-trivial as the radii need to include the "bound" hydration shells of ions. While there are measured values available for many ions, whether and how much ions retain their hydration shells within the DNA arrays are not clear. We thus chose 2 Å as a reasonable approximation. The results shown in (b)-(d) further indicate that an error of ±1 Å affects the predictions by 5% or much less, thus not compromising our conclusions.

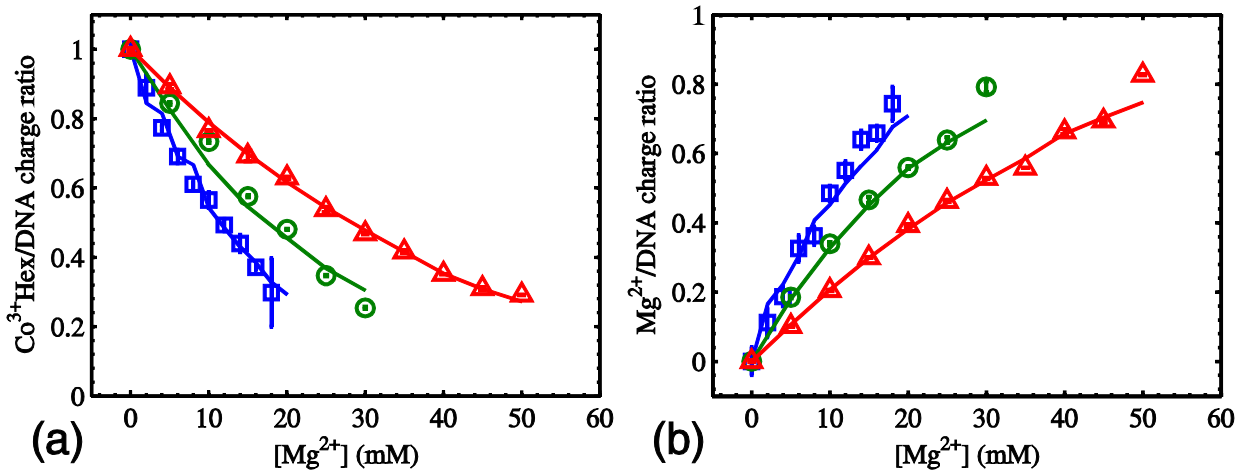

Figure S5. Measured ion/DNA charge ratios compared with the cylindrical cell model (CCM) calculations. Symbols are the same experimental data as in Fig. 2 in the main text (i.e., ion/DNA charge ratios at fixed $[Co^{3+}Hex]$s of 1 mM (□), 2 mM (○) and 5 mM (Δ) and varied $[Mg^{2+}]$s as the x axis). The solid lines in matched colors are the CCM predictions using a dissociation constant of K_d=120 mM for the ion paring reaction $Co^{3+}Hex + Cl^- \leftrightarrow Co^{3+}HexCl^-$.

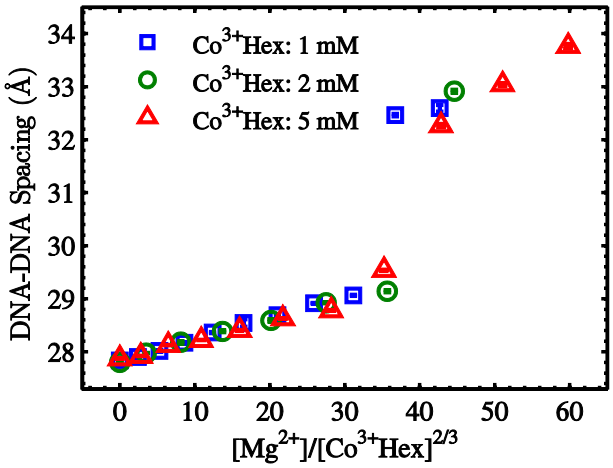

Figure S6. The convergence of the DNA-DNA spacing on the reduced variable of the bath solution, $[Mg^{2+}]/[Co^{3+}Hex]^{2/3}$. Symbols are the same experimental data as in Fig. 3 with nominal $[Co^{3+}]$s indicated by the legends.